Cu–ATSM: A radiopharmaceutical for the PET imaging of hypoxia†

Amy L. Vāvere and Jason S. Lewis*

Received 23rd April 2007, Accepted 18th June 2007
First published as an Advance Article on the web 25th September 2007
DOI: 10.1039/b705989b

Copper(II)-diacetyl-bis(N^4-methylthiosemicarbazone), Cu–ATSM, labeled with a positron emitting isotope of copper (^{60}Cu, ^{61}Cu, ^{62}Cu or ^{64}Cu) has been shown, *in vitro* and *in vivo*, to be selective for hypoxic tissue. *In silico* studies have explored the mechanism of its hypoxia selectivity, and clinical studies with this agent have shown non-invasive imaging data that is predictive of a cancer patients' response to conventional therapy. This Perspective discusses the evolution of Cu–ATSM, how its selectivity can be improved upon, and where this metal–ligand platform could be taken in the future.

Introduction

The onset of hypoxia in malignant tissues is associated with and influenced by a myriad of complicated physiological processes. Increase in tumour aggressiveness, failure of local control, and metastatic potential of solid tumours are believed to be highly associated with the presence of hypoxia within the cancer.[1] Determining the extent of tumour hypoxia in solid cancers is important in monitoring response to radiotherapy, since tumour cells become radioresistant at low oxygen tension.[1] In addition, tumour hypoxia is associated with resistance to chemotherapy and with increased tumour aggressiveness, manifested as a higher rate of recurrence and metastasis.[2–4]

To review the consequences of tumour hypoxia, its importance in tumour biology, measurement, management, and the non-invasive approaches to measure tissue hypoxia, the reader is referred to a recent comprehensive review.[5] In general normal tissues exhibit a Gaussian partial pressure of oxygen (pO_2), with a median value of the resting heart at 17 mmHg and 65 mmHg in the spleen and breast. In solid tumours this Gaussian pO_2 shifts to significantly lower values often to the point of anoxia (0 mmHg). The level at which hypoxia in human cancers becomes clinically significant often depends on the cancer type and the method of measurement. In 103 patients with cervical cancer, a pO_2 of 10 mmHg was used as a cutoff to define significant differences in disease free survival, independent of tumour stage.[3] A similar study on 106 patients defined a similar cutoff but with a pO_2 at 5 mmHg.[6] In studies of head and neck cancer, hypoxia measurement was also prognostic for outcome but the cutoff typically involved pO_2 levels

Department of Radiology, Mallinckrodt Institute of Radiology, and the Alvin J. Siteman Cancer Center, Washington University School of Medicine, Campus Box 822, 5510 South Kingshighway Blvd, St. Louis, MO, 63110, USA. E-mail: j.s.lewis@wustl.edu; Fax: +1 314 362 9940; Tel: +1 314 362 4696

† Based on the presentation given at Dalton Discussion No. 10, 3rd–5th September 2007, University of Durham, Durham, UK.

Dr Vāvere earned her B.S. in Chemistry from Drake University in 1998. In 2004 she graduated with a Ph.D. in Chemistry from Washington University under the direction of Professor Michael J. Welch. Her graduate work focused on the development of ^{45}Ti radiopharmaceuticals. She then joined the Lewis laboratory and with support from an NIH/NRSA postdoctoral fellowship she has been studying the use of radiopharmaceuticals for the monitoring of cancer therapy by applying multi-modality imaging.

Amy L. Vāvere

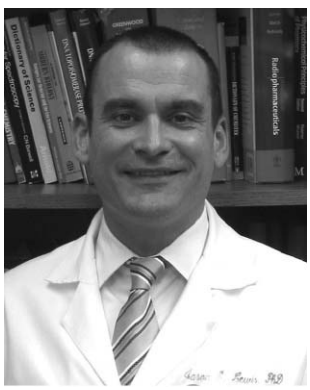

Jason S. Lewis

Dr Lewis earned a B.Sc. (Hons) in Chemistry (1992) and a M.Sc. (1993) in Chemistry from the University of Essex in the laboratory of Professor Jonathan R. Dilworth. He received a Ph.D. in Biochemistry in 1996 from the University of Kent mentored by Professor Philip J. Blower. After his postdoctoral work with Professors Carolyn J. Anderson and Michael J. Welch at the Mallinckrodt Institute of Radiology at Washington University School of Medicine, he joined the faculty as an Assistant Professor of Radiology in 2003. His areas of interest include the cyclotron production of metallic PET radionuclides and the use of radiopharmaceuticals for the delineation of cancer. The Lewis lab utilizes small animal imaging (PET, CT and MRI) for their research, and he is the Co-Operations Director of the Small Animal PET facility of WUSM. Dr Lewis has co-authored over 75 articles, reviews and chapters. Dr Lewis' laboratory is supported by grants from the United States Department of Defense and the National Institutes of Health.

of 2.5 mmHg.[7] Over the past 15 years, pO_2 values of <2.5 mmHg have been shown to become a physiological property of locally advanced solid tumours.[8] In general, however, these studies were performed with an oxygen needle electrode, which is an invasive technique that can be fraught with sampling errors, that requires accessibility to the tumour, and is therefore not applicable for all tumour types.

In recent decades, investigations into alternative, non-invasive imaging methods for measuring pO_2 have been pursued by numerous researchers. The use of positron emission tomography (PET), in conjunction with radiolabeled molecules that undergo chemical changes in the presence or absence of oxygen, has led to a number of promising agents which have all been reviewed in detail.[5,9–14] An imaging method for *in vivo* measurement of tissue hypoxia with nitroimidazoles has been developed. These compounds are known to undergo different intracellular metabolism depending on the availability of oxygen in the tissue. The most widely studied nitroimidazole for *in vivo* PET imaging is [^{18}F]fluoromisonidazole (^{18}F-FMISO) (Fig. 1). Based on prior characterization of oxygen dependence on ^{18}F-FMISO binding, hypoxic regions must have pO_2 levels below 2–3 mmHg (~2600–4000 ppm, where 1 mmHg = 1317 ppm) to cause substantial retention.[15]

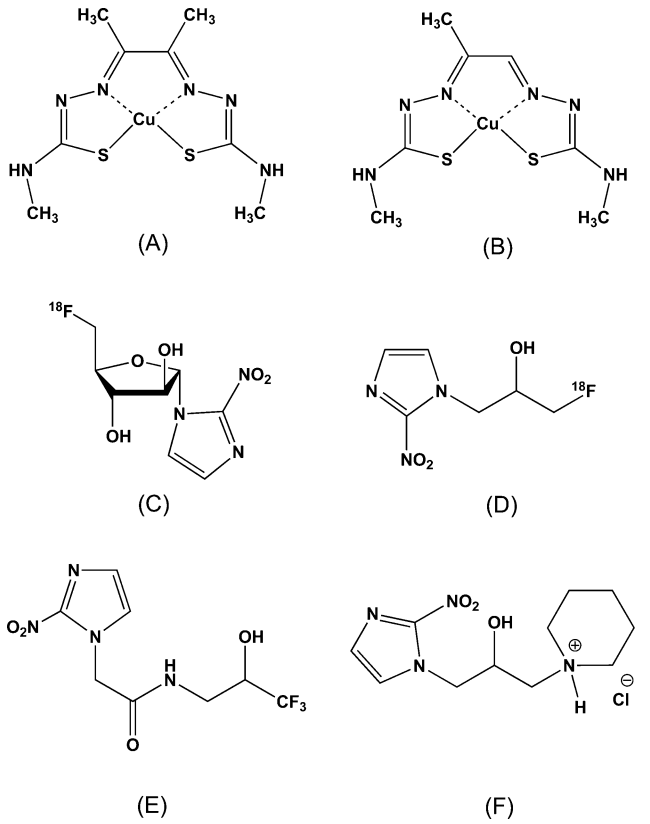

Fig. 1 (A) Cu(II)-diacetyl-bis(N^4-methylthiosemicarbazone), or Cu–ATSM; (B) Cu-pyruvaldehyde-bis(N^4-methylthiosemicarbazone), or Cu–PTSM; (C) ^{18}F-fluoroazomycin arabinoside, or ^{18}F-FAZA; (D) [^{18}F]fluoromisonidazole, or ^{18}F-FMISO; (E) [2-(2-nitro-1*H*-imidazol-1-yl)-*N*-(2,2,3,3,3-pentafluoropropyl) acetamide], or EF5 and; (F) pimonidazole hydrochloride (Hydroxyprobe™).

Although many studies have demonstrated that an *in vivo* assessment of tumour hypoxia is possible with ^{18}F-FMISO,[16–18] the unfavorable imaging characteristics of this compound have somewhat limited its wider usage in clinical oncology. The main advantage of ^{18}F-FMISO is that it is directly affected by tumour oxygenation, however, there are two major limitations with ^{18}F-FMISO imaging. One is the limited contrast ratio between hypoxic tumours and normal tissues (tumour to blood ratio > 1.2) reflecting the relatively low tissue uptake of ^{18}F-FMISO *in vivo*.[17–19] The other is the slow cellular washout of this tracer; a delay of approximately 2 h after injection of ^{18}F-FMISO is needed to permit clearance of this tracer from normal background tissues. This delays imaging and results in low-count-rate studies and images of limited quality.[16,17,19] Other nitroimidazole-based ^{18}F-radiopharmaceuticals have been investigated,[16] with ^{18}F-fluoroazomycin arabinoside (^{18}F-FAZA) (Fig. 1) being the most recently studied as it shows similar uptake as ^{18}F-FMISO but with better blood clearance.[20] This study also verified a hypoxia-specific uptake mechanism for ^{18}F-FAZA in murine tumour models.

The focus of this Perspective is on copper(II)-diacetyl-bis(N^4-methylthiosemicarbazone), or Cu–ATSM (Fig. 1), a PET agent that has been developed as an alternative to ^{18}F-FMISO, overcoming many of its limitations. Cu–ATSM is an agent that shows rapid delineation of tumour hypoxia (< 1 h) and in high tumour to background tissue ratios (tumour to blood ratios ≫2.0). This agent has been translated from the bench to the clinic by biologists, chemists, physicists and physicians from all over the world.

Copper and copper positron-emitting nuclides

The use of copper radionuclides presents many advantages over other more established metal radionuclides such as ^{99m}Tc. The chemistry of copper is restricted to two principle oxidation states (I and II), and the relatively simple coordination and redox chemistry of copper is well documented. Also, since copper is ubiquitous in nature, its biochemistry and metabolism in humans is relatively well known. The increasing availability and broader dissemination of positron-emitting isotopes of copper make them attractive options on which to base new positron-emitting radiopharmaceuticals.

The positron-emitting isotopes of copper (^{60}Cu, ^{61}Cu, ^{62}Cu and ^{64}Cu) are particularly versatile given their range of decay schemes [^{60}Cu ($t_{1/2}$ = 0.40 h, β^+ = 93%, EC = 7%); ^{61}Cu ($t_{1/2}$ = 3.32 h, β^+ = 62%, EC = 38%); ^{62}Cu ($t_{1/2}$ = 0.16 h, β^+ = 98%, EC = 2%); and ^{64}Cu ($t_{1/2}$ = 12.7 h, β^+ = 17.4%, EC = 43%)].[21–23] Copper-60, ^{61}Cu and ^{64}Cu can be produced in high specific activity on small cyclotrons using reliable and reproducible targetry methods.[24,25] The preparation of ^{62}Cu, *via* a ^{62}Zn/^{62}Cu generator system, has been reported and commercialized.[26,27] Copper-64 is the most commonly used copper isotope, and its production and use has now been reported in the United States, Europe and Japan.[25,28–31] With a half-life of 12.7 h, it is ideally suited for PET studies that can be conducted over a 48 hour period. This longer half-life also allows for the distribution of this nuclide, as with ^{18}F, from regional production centers to imaging centers that may not have direct access to a cyclotron. Copper-64 decays 17.4% by positron emission and has a β+ maximum energy of 0.66 MeV with an average energy of 0.28 MeV. Copper-64 also decays by electron capture (43%) and β−(43%) and has, therefore, been studied as both a diagnostic and therapeutic radionuclide.[21] Since ^{64}Cu has

a β+ maximum energy of 0.66 MeV, similar to ^{18}F, the resulting PET images are of very high quality.

Copper–ATSM

Dithiosemicarbazones were discovered to possess anti-tumour properties in the 1960's, and it was further found that the anti-tumour activity of the Cu(II) complexes of these ligands was significantly enhanced over the activity of the ligands alone.[32,33] This led to the exploitation of this class of ligands as radiopharmaceuticals due to the simplicity of the chemistry and the availability of the copper PET isotopes. The basic science and clinical exploration of radiopharmaceuticals based on copper–thiosemicarbazones was first initiated around the development of agents to measure blood flow, *e.g.*, Cu-pyruvaldehyde-bis(N^4-methylthiosemicarbazone) (Cu–PTSM) (Fig. 1).[34–36] This research later evolved over years into agents to delineate other biological processes such as hypoxia. The first report of the hypoxia-selectivity of Cu–ATSM was in an isolated rat heart model of ischemia in 1997.[37]

In vitro

Following the first report of Cu–ATSM as an agent for selectively delineating hypoxic myocardial tissue,[37] Dearling *et al.* undertook a systematic *in vitro* study comparing 13 ^{64}Cu–bis(thiosemicarbazone) (Table 1) complexes for tumour hypoxia selectivity.[38] The complexes were incubated with CHO320 cells under both normoxic and anoxic conditions, and several members (5/13) of the ^{64}Cu–bis(thiosemicarbazone) series demonstrated significant hypoxia selectivity, including ^{64}Cu–ATSM. The addition of a second methyl group on the diimine backbone of the ligand alone resulted in the hypoxia-selectivity of Cu–ATSM, compared to non-selectivity of Cu–PTSM.[39] This initial study elegantly demonstrated that the hypoxia selectivity of the copper complexes could be achieved by subtle manipulation of the ligand.

In 1999, the *in vitro* kinetics of ^{64}Cu–ATSM in EMT6 cells were compared to ^{18}F-FMISO, the misonidazole drug described earlier.[40] In addition, the *in vivo* biodistribution of ^{64}Cu–ATSM was compared to that of the flow tracer ^{64}Cu–PTSM in EMT6 tumour-bearing mice. Uptake of ^{64}Cu–ATSM, ^{64}Cu–PTSM and ^{18}F-FMISO into EMT6 cells was investigated at the dissolved oxygen concentrations of 0 (anoxia), 1×10^3, 5×10^3, 5×10^4 and 2×10^5 (normoxia) ppm. These dissolved concentrations were confirmed with an oxygen electrode that measured the dissolved oxygen concentration of the incubation media. After 1 h, ^{64}Cu–ATSM was taken up by cells: 90% at 0 ppm O_2, 77% at 1×10^3 ppm, 38% at 5×10^3 ppm, 35% at 5×10^4 ppm and 31% at 2×10^5 ppm, showing nearly a three-fold higher retention of ^{64}Cu–ATSM in severely hypoxic cells compared to normal oxygenated cells (Fig. 2). This study showed a sigmoidal inflection (*i.e.*, the threshold of selectivity) between 5×10^3 (3.8 mmHg) and

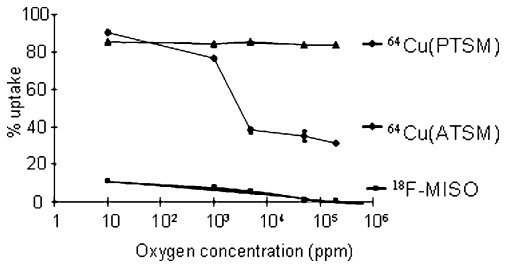

Fig. 2 Percentage uptake of ^{64}Cu–ATSM, ^{64}Cu–PTSM and ^{18}F-FMISO into EMT6 cells over time at varying oxygen concentrations, 0, 1×10^3, 5×10^3, 5×10^4 and 2×10^5 ppm in the cell media. Reprinted by permission of the Society of Nuclear Medicine from: J. S. Lewis, D. W. McCarthy, T. J. McCarthy, Y. Fujibayashi, M. J. Welch. Evaluation of ^{64}Cu-ATSM In Vitro and In Vivo in a Hypoxic Tumor Model. *J. Nucl. Med.*, 1999, **40**(1), 177–183, Figure 2.

Table 1 Physiochemical and hypoxia selectivity properties of the Cu–bis(thiosemicarbazone) complexes[38,39,51]

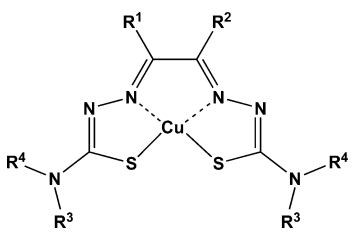

Complex	R^1	R^2	R^3	R^4	Log*P*	$E_{1/2}$ Cu(II/I)/ V (*vs.* Ag/AgCl)	Selectivity in CHO320 cells
Cu–GTS	H	H	H	H	0.45	−0.43	Normoxia (significant)
Cu–GTSM	H	H	CH_3	H	0.84	−0.43	Normoxia (significant)
Cu–PTS	CH_3	H	H	H	0.53	−0.50	Not significant
Cu–PTSM	CH_3	H	CH_3	H	1.45	−0.51	Hypoxia (significant)
Cu–$PTSM_2$	CH_3	H	CH_3	CH_3	2.35	−0.53	Not significant
Cu–PTSE	CH_3	H	C_2H_5	H	1.96	−0.52	Normoxia (significant)
Cu–PTSP	CH_3	H	C_6H_5	H	1.96	−0.31	Not significant
Cu–ATS	CH_3	CH_3	H	H	0.65	−0.59	Not significant
Cu–ATSM	CH_3	CH_3	CH_3	H	1.48	−0.59	Hypoxia (highly significant, $P < 0.0001$)
Cu–CTS	C_2H_5	CH_3	H	H	2.34	−0.59	Hypoxia (highly significant, $P = 0.00095$)
Cu–CTSM	C_2H_5	CH_3	CH_3	H	2.69	−0.58	Not significant
Cu–DTS	C_2H_5	C_2H_5	H	H	1.69	−0.59	Hypoxia (highly significant, $P < 0.0001$)
Cu–DTSM	C_2H_5	C_2H_5	CH_3	H	2.34	−0.58	Hypoxia (highly significant, $P = 0.0026$)

1×10^3 ppm (0.8 mmHg) of dissolved O_2 which is centered around pO_2 levels of tumour hypoxia (2–3 mmHg). ^{18}F-FMISO also showed oxygen concentration dependent uptake, but with lower percentages than ^{64}Cu–ATSM, and ^{64}Cu–PTSM showed 83–85% uptake into the cells after 1 h, independent of O_2 concentration. Compared to ^{18}F-FMISO, Cu–ATSM exhibited more efficient uptake and superior washout kinetics in hypoxic and normoxic cells offering the possibility of a superior means of detecting tumour hypoxia by PET imaging.

In 2005, Burgman *et al.*, showed that the uptake and retention of ^{64}Cu–ATSM, and their relation to the levels of cellular oxygenation was found to be cell line dependent.[41] Four tumour cell lines of human origin and two of rodent origin were studied. Moreover, it was demonstrated that there was considerable variation in ^{64}Cu accumulation, with uptake in normoxic cells being anywhere from two to nine times lower that than in hypoxic cells depending on the cell line and incubation time. One cell line, a rat prostate tumour line R3327-AT, did not show any hypoxia selectivity, and a possible explanation of this is discussed later.

In vivo

In 1999, a comparative biodistribution of ^{64}Cu–ATSM with ^{64}Cu–PTSM in BALB/c mice bearing EMT6 tumours was reported.[40] The biodistribution data of ^{64}Cu–ATSM and ^{64}Cu–PTSM showed optimal tumour uptake after 10 min post-injection, suggesting a rapid trapping mechanism for Cu–ATSM in solid tumours. *Ex vivo* autoradiography of tumour slices following co-injection of ^{60}Cu–PTSM and ^{64}Cu–ATSM into the same animal showed ^{60}Cu–PTSM uniform throughout the EMT6 tumour but heterogeneous uptake of ^{64}Cu–ATSM, indicative of trapping of ^{64}Cu–ATSM into the 'hypoxic' regions of the tumours. Using oxygen needle electrode measurements of the solid tumour, PET and electronic autoradiography, a strong relationship between low tumour pO_2 and high Cu–ATSM accumulation was observed in 9L gliosarcomas tumours in rats.[42] By chemical manipulation of tumour pO_2, a significant increase in Cu–ATSM was observed in hypoxic-induced tumours. This was the first study confirming that Cu–ATSM uptake in cancerous tissues *in vivo* was dependent upon the tissue pO_2.

With the advent of small animal PET imaging technology, a very careful comparison was made between tumour bearing rats that were administered ^{64}Cu–ATSM and ^{18}F-FMISO to assess the regional distribution of the two tracers, and to correlate their uptake to each other as well as direct pO_2 tumour measurements, autoradiography, and fluorescent microscopy.[43] In Fisher–Copenhagen rats bearing the R3327-AT anaplastic rat prostate tumour, there was a poor correlation between the intra-tumoural distribution of ^{18}F-FMISO and ^{64}Cu–ATSM except at later times (16–20 h pi). ^{18}F-FMISO and ^{64}Cu–ATSM microPET images were also acquired in nude rats bearing xenografts derived from the human squamous cell carcinoma cell line, FaDu. For the FaDu tumour model, the early and late ^{64}Cu–ATSM microPET images were similar and were in general concordance with the ^{18}F-FMISO scans.

In an effort to better characterize the hypoxia-selectivity of Cu–ATSM and the relationship of its distribution to other prominent physiological tumour characteristics, studies have been undertaken comparing ^{64}Cu–ATSM with ^{18}F-fluorodeoxyglucose (^{18}F-FDG), an agent for measuring tumour glucose metabolism.[42,44,45] In general it was shown that ^{64}Cu–ATSM and ^{18}F-FDG were distributed with different graduations within animal tumours. Conclusions showed that regions of high ^{18}F-FDG uptake were actively proliferating, as confirmed by histological analysis with Ki67, and may respond well to conventional treatments.[45] In contrast, regions of high ^{64}Cu–ATSM were viable, but hypoxic and may be resistant to treatment.

One of the most important validation studies of Cu–ATSM as an agent for delineating hypoxia was reported in 2006 by Yuan *et al.*[46] The authors compared the autoradiographic distributions of ^{64}Cu–ATSM with a well-established hypoxia marker drug (EF5, Fig. 1) in R3230 mammary adenocarcinomas, fibrosarcomas (FSA), and 9L gliomas. They demonstrated that a significantly higher T/M (tumour/muscle) ratio and SUV (standardized uptake value) were seen for FSA compared with R3230Ac and 9L and that a spatial correlation analysis between ^{64}Cu–ATSM autoradiography and EF5 images varied between the 3 tumour types. There was close correlation of ^{64}Cu–ATSM uptake and hypoxia in R3230Ac and 9L tumours, but not in FSA tumours. The same relationship was observed with 2 other hypoxia markers, pimonidazole (Fig. 1) and carbonic anhydrase IX, in FSA tumours. This study confirmed that ^{64}Cu–ATSM is a valid PET hypoxia marker in most tumour types, but not for all, and suggested that ^{64}Cu–ATSM may not act as a universal PET hypoxia marker.

Structure and mechanism

The retention mechanism of Cu–ATSM has been hypothesized and explored by a number of groups in the US, Europe and Japan.[35,38,39,41,47–54] The premise for bioreductive hypoxia selectivity was based on the discovery of bioreductive trapping of Cu–PTSM and related complexes in the early 1990's.[55,56] The redox activity of the copper(II) bis(thiosemicarbazones) complexes was correlated to their structure–activity relationships in 1998.[51] The reduction potential and lipophilicity of the Cu–bis(thiosemicarbazones) was controlled by the alkylation of the ligand backbone, which allowed for optimization of their uptake into hypoxic tumour cells.[38] Further, it was shown that the redox potential was not the only factor controlling hypoxia selectivity: although complexes with potentials in the range −0.57 to −0.59 V were all hypoxia selective, they differed in the degree of selectivity.[51] Two major mechanisms have been proposed, but they are not mutually exclusive and may be different aspects of the same overall mechanism.

A proposed mechanism of Cu–ATSM retention was first reported by Fujibayashi *et al.*, where it was suggested that Cu(II)–ATSM reduction only occurred in hypoxic cells and was then irreversibly trapped.[37] Obata *et al.*, compared the retention mechanism of Cu–ATSM in tumour cells with that in normal tissue.[54] With Cu–ATSM and reversed phase HPLC analysis, the reductive metabolism of Cu–ATSM in subcellular fractions obtained from tumour cells was examined. In subcellular fractions studies, Cu–ATSM was reduced mainly in the microsome/cytosol fraction rather than in the mitochondria. The reduction process in the microsome/cytosol was heat-sensitive and enhanced by adding exogenous NADPH, an indication of enzymatic reduction of Cu–ATSM in tumour cells. Moreover, it was also shown that the bioreductive enzymes, NADH-cytochrome b5 reductase and NADPH-cytochrome P450 reductase in the microsomes played a major role in the reductive retention of Cu–ATSM in tumours,

and that this enzymatic reduction was enhanced by the induction of hypoxia.

Additional studies on the mechanism of Cu–ATSM retention were reported by Dearling *et al.*,[39] and Maurer *et al.*[53] These reports suggested that reduction of Cu(II)–ATSM took place in both normoxic and hypoxic cells resulting in unstable Cu(I)–ATSM. This unstable species would slowly dissociate, and if completely dissociated (in hypoxic cells) it would be irreversibly trapped, but in the presence of oxygen (normoxic cells) the Cu(I)–ATSM would be reoxidized to Cu(II)–ATSM and diffuse back out of the cell. Blower *et al.* focused on the fate of the reduced Cu(I) state using a combination of density functional calculations, cyclic voltammetry over a range of pH, and UV/visible spectroscopic monitoring of redox reactions.[48,53] Additional insight into the contribution of the electronic structure was also provided by comparisons between the copper complexes of the sulfur-containing bis(thiosemicarbazones) and their selenium analogs.[57] The data strongly suggested that the hypoxia selectivity of the Cu–ATSM complex depends on the stability of the Cu(I) species. The chemical and electrochemical results in these studies supported the hypothesis that intracellular reduction of the Cu(II) bis(thiosemicarbazone) complexes can lead to two distinct patterns of chemical behavior: rapid acid-catalyzed dissociation (non-hypoxia-selective complexes Cu–GTS, Cu–PTSM, *etc.*) or resistance to dissociation allowing subsequent reoxidation by molecular oxygen, if present (hypoxia-selective complexes, Cu–ATSM, *etc.*). This hypothesis is consistent with previously reported uptake–washout experiments.[38–41,51]

As stated in the discussion on the *in vitro* data and later in the discussion of the clinical data, the imaging of hypoxia may be considerably variable based on tumour type. In order to help understand the implications of this issue with Cu–ATSM imaging, additional studies on the fundamental chemistry of the H_2ATSM ligand should be performed to deconvolute the redox chemistry from the basic coordination chemistry. A recent study with Zn–ATSM begins, in part, to resolve this issue.[58] The uptake of zinc bis(thiosemicarbazone) complexes in human cancer cells was studied by fluorescence microscopy and the cellular distribution established, including the degree of uptake in the nucleus. This study showed that Zn–ATSM is internalized by cells and differentially compartmentalized within cells as seen by the intrinsic fluorescence of the complex. Moreover, it also demonstrated that the distribution within the cytoplasm depends on the cell type. Since the structures of the zinc complexes are very similar to their copper analogues, the cell uptake mechanisms may well be similar. This report demonstrated clearly that uptake in the nucleus was a sensitive function of the terminal nitrogen substituents on the complexes and that the integrity of the complexes was maintained. As Zn is not redox active like Cu, these data, and studies like it, could help to further elucidate the mechanism of Cu–ATSM accumulation and retention.

The crystal structure of Cu(II)–ATSM was determined for the first time in 2002 (Fig. 3A),[49] but it was not possible to isolate the Cu(I) species for comparison. The researchers did, however, isolate the novel dimeric species $[Cu_2(ATSMH_2)_2]^{2+}$. The X-ray crystal structure of this agent (Fig. 3B) revealed a dimeric structure with each of the ATSM ligands acting as a bidentate N–S donor to each Cu(I) ion to generate a novel helical structure which was unprecedented for bis(thiosemicarbazone) complexes. The authors suggested that this dimer may be formed in cells following uptake. Cyclic voltammetry studies showed clearly that reduction of the [Cu(II)(ATSM)] complex in the mildly acidic aqueous environment inside a cell would be accompanied by protonation and generate an unstable diprotonated Cu(I) cation. Whatever the precise identity of this species, it is retained, possibly by virtue of the positive charge, and is rapidly re-oxidized by oxygen in normoxic cells to regenerate the planar Cu(II)–ATSM complex which diffuses out of the cell. Additional support for Cu(I)–$ATSMH_2^+$ being the initial species trapped in hypoxic cells, was provided by DFT calculations of the redox potentials and absolute acidities of the complex in solution.[52] A second solving of the crystal structure of Cu–ATSM, along with seven other bis(thiosemicarbazone) analogs was reported in 2003.[47]

Cu–ATSM: Patient studies

The first report of Cu–ATSM evaluated in humans was published in 2000 by a Japanese group in patients with lung cancer.[59] The imaging characteristics of ^{62}Cu–ATSM were observed in 4 normal subjects and 6 patients with lung cancer. An intense uptake of ^{62}Cu–ATSM was observed in all the cancer patients, and a negative correlation was observed between flow and flow-normalized ^{62}Cu–ATSM uptake.

The first correlative studies comparing ^{60}Cu–ATSM uptake in tumours with the response of the tumour to conventional therapies were published in 2003.[60,61] In both studies ^{60}Cu–ATSM showed high contrast levels between hypoxic and normoxic tissues by as little as 10–15 min post injection and yielded clinically relevant information about tumour oxygenation that was predictive of tumour behavior and response to therapy. Data was based on 30–60 min of summed data from the imaging session. In a prospective study of 14 humans with non-small cell lung cancer, a

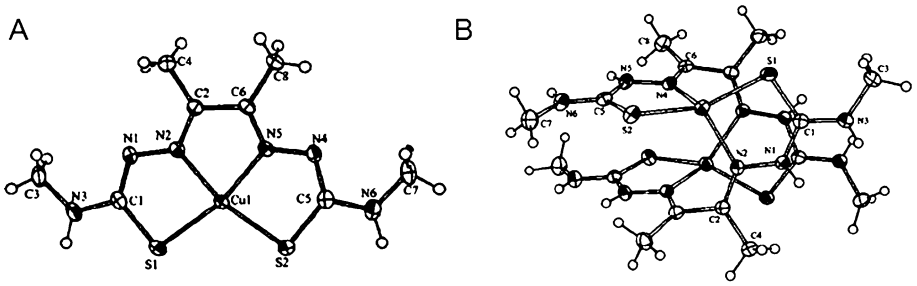

Fig. 3 (A) Crystal structure of [Cu(II)(ATSM)]. (B) Crystal structure of the dimeric species $[Cu_2(ATSMH_2)_2]^{2+}$. Reprinted with permission from A. R. Cowley *et al.*, *J. Am. Chem. Soc.*, 2002, **124**, 5270–5271. Copyright 2002 American Chemical Society.

semi-quantitative analysis of the ^{60}Cu–ATSM tumour-to-muscle ratio (primary lung cancer *vs.* bilateral back muscle groups) was able to discriminate those likely to respond to therapy from non-responders (Fig. 4).[61] The tumour/muscle ratio for ^{60}Cu–ATSM was significantly lower in responders (1.5 ± 0.4) than in non-responders (3.4 ± 0.8) ($P = 0.002$), suggesting low ^{60}Cu–ATSM uptake was indicative of normoxic tumour whereas higher ^{60}Cu–ATSM uptake suggested tumour hypoxia. The maximum standardized uptake value (SUV_{max}) was also determined for ^{60}Cu–ATSM. However, there was no significant difference in mean tumour SUV of non-responders (3.5 ± 1.0) and responders (2.8 ± 1.1) (p = 0.2). Tumour SUV values for ^{18}F-FDG were not significantly different in responders and non-responders ($P > 0.7$) and did not correlate with ^{60}Cu–ATSM uptake ($r = 0.04$; $P = 0.9$). A study in 14 women with cervical cancer demonstrated a similar predictive value in the tumour response to therapy (Fig. 5).[60] An arbitrarily selected tumour/muscle threshold of 3.5 discriminated those likely to develop tumour recurrence; 6 of 9 patients with normoxic tumours (tumour/muscle < 3.5) were free of disease, whereas all of the 5 patients with hypoxic tumours (tumour/muscle > 3.5) had developed recurrence at the end of the study. Tumour ^{18}F-FDG uptake did not correlate with ^{60}Cu–ATSM uptake ($r = 0.04$; $P = 0.80$). To determine if hypoxia-related molecular markers were associated with ^{60}Cu–ATSM retention, the PET imaging data of the patients with cancer of the cervix were compared with the expression of tissue molecular markers, which included vascular endothelial growth factor (VEGF), cyclo-oxygenase-2 (COX-2), epidermal growth factor receptor (EGFR), carbonic anyhdrase IX (CA-9), and apoptotic index. Overexpression of VEGF ($p = 0.13$), EGFR ($p = 0.05$), CA-9 ($p = 0.02$), COX-2 ($p = 0.08$), and the presence of apoptosis ($p = 0.005$) occurred in patients with hypoxic tumours.[62]

Having shown the ability of Cu–ATSM to delineate hypoxic regions of tumours, a feasibility study was performed to determine if the PET image information could be used to plan a patients' course of radiotherapy.[63] Given the resistance of hypoxic tumours to radiotherapy, determining the level and location of hypoxia within a tumour could be used to perform intensity-modulated radiation therapy (IMRT) by delivering a higher dose of radiation to hypoxic regions of the tumour while protecting the healthy margin. In 2001, Chao *et al.*, demonstrated this approach by co-registering PET/CT data for IMRT planning in head and neck cancer patients.[63]

With these studies completed, the imaging data was used to determine the absorbed radiation doses for Cu–ATSM labeled with ^{60}Cu, ^{61}Cu, ^{62}Cu and ^{64}Cu.[64] These doses were estimated from both rat biodistribution and the direct imaging measurement in 5 patients that underwent ^{60}Cu–ATSM imaging. Based on the human PET imaging data, the liver appeared as the dose-limiting

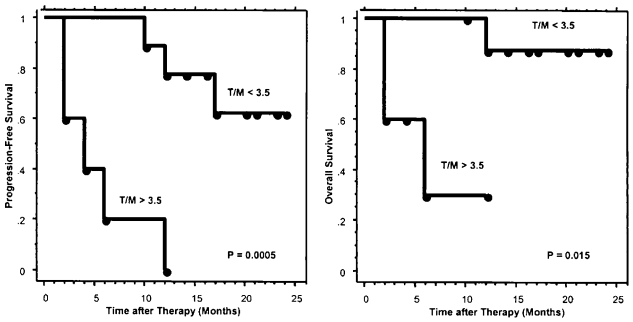

Fig. 5 Progression-free survival and overall survival based on ^{60}Cu–ATSM uptake using Kaplan–Meier method. Patient survival has an inverse relationship with tumour uptake of ^{60}Cu–ATSM assessed by tumour-to-muscle activity ratio ($p = 0.0005$ and $p = 0.015$, respectively). Reprinted from *Int. J. Radiat. Oncol. Biol. Phys.*, **55**, Dehdashti *et al.*, Assessing Tumor Hypoxia in Cervical Cancer by Positron Emission Tomography with ^{60}Cu-ATSM: Relationship to Therapeutic Response - A Preliminary Report, 1233–1238, Copyright 2003, with permission from Elsevier Inc.

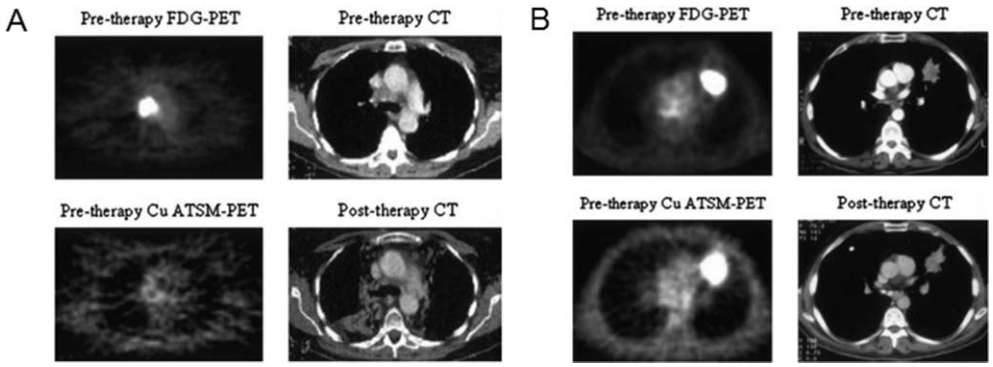

Fig. 4 (A) Responder. Transaxial FDG-PET image (upper left) of the chest shows moderately intense FDG uptake (SUV 4.9) in the known lung cancer. Transaxial ^{60}Cu–ATSM-PET image (lower left) at the same level demonstrates minimal uptake within the tumour (T/M = 1.3). CT image prior to therapy (upper right) demonstrates increased soft tissue density in the precarinal space, consistent with patient's known cancer. CT image after radiotherapy (lower right) demonstrates post-radiation changes, but shows a good response of the tumour to the treatment. The patient was alive at last follow-up (46 months after the diagnosis of lung cancer) without evidence of tumour recurrence. (B) Non-responder. Transaxial FDG-PET image (upper left) of the chest shows intense FDG uptake (SUV 17.3) in the known lung cancer in the lingula. Transaxial ^{60}Cu–ATSM-PET image (lower left) at the same level demonstrates intense uptake within the lingular cancer (T/M = 3.0). CT image prior to therapy (upper right) demonstrates a lingular mass, consistent with patient's known lung cancer. CT image (lower right) 3 months later, during chemotherapy demonstrates an increase in the size of the tumour. The patient died with progressive disease 15 months after diagnosis. Reprinted from Springer-Verlag. Copyright 2003/*Eur. J. Nucl. Med Mol. Imaging*, **30**, 2003, 844–850, *In vivo* assessment of tumour hypoxia in lung cancer with ^{60}Cu-ATSM, Dehdashti *et al.*, Figures 2 and 3. With kind permission from Springer Science and Business Media.

organ with an average radiation dose of 0.064 mGy MBq^{-1} from ^{60}Cu–ATSM, with a whole-body dose of 0.009 mGy MBq^{-1}, and an effective dose of 0.011 mSv MBq^{-1}. When extrapolated to ^{64}Cu–ATSM the liver would have an average radiation dose of 0.390 mGy MBq^{-1}, with a whole-body dose of 0.026 mGy MBq^{-1}, and an effective dose of 0.036 mSv MBq^{-1}.

With this information on hand, and support from the DCIDE program at the National Cancer Institute at the United States National Institutes of Health to generate the pharmacology and toxicity data for Cu–ATSM, the FDA approved a pilot study in 2006 (IND 62,675) examining the uptake and kinetics of ^{64}Cu–ATSM in women with cancer of the uterine cervix. This will likely lead to a multi-center trial within the United Sates. With production of ^{64}Cu in Japan and Europe, it is likely that additional clinical trials with ^{64}Cu–ATSM will be initiated soon in these countries.

Other applications

New directions

The use of Cu–ATSM for predicting the response of a cancer patient's tumour to conventional therapy is perhaps the primary clinical application of Cu–ATSM. However, it could also be used for monitoring therapies directed at modulating a tumour prior to treatment. For example, mild hyperthermia can improve tumour oxygenation and enhance radiosensitivity. Imaging the hypoxic fraction of a tumour could guide hyperthermia treatment planning (similar to IMRT) and facilitate an effective treatment of the disease. Myerson *et al.*, were able to use Cu–ATSM to discriminate the effects of mild hyperthermia on tumour physiology in animal tumour models with a view to treatment planning.[65] In 2006, Rust and Kadrmas, reported a simulation study on a rapid dual-tracer Cu–PTSM/Cu–ATSM PET imaging of tumour flow and hypoxia,[66] that when combined with treatments such as hyperthermia could resolve hypoxic uptake from blood flow, helping to further personalize therapies to overcome resistance in tumours.

Therapeutic applications

When complexed with a larger amount of ^{64}Cu, given the therapeutic properties of the ^{64}Cu nuclide, copper–thiosemicarbazone agents (Cu–ATSM and Cu–PTSM) have also been described as potential therapeutics based on their biological and nuclear properties.[67–70] Since ^{64}Cu decays 43% by electron capture, it emits Auger electrons with high LET. ^{64}Cu emits a 6.84 keV Auger electron with a penetration range of about 5 μm, the approximate cell nucleus diameter. Moreover, the maximum recoil energy from the transmutation of ^{64}Cu (from $\beta- = 7.6$ eV; from $\beta+ = 9.15$ eV) to its highly charged daughter nucleus may also increase the cell killing ability. The combination of these characteristics with the likely event ^{64}Cu is bound to certain structures within the nucleus increase its toxicity. Additionally, Auger- and recoil-linked toxicity would be as great in hypoxic cells as in oxygenated. In 2001, it was reported that the systemic administration of ^{64}Cu–ATSM significantly increased the survival time of hamsters bearing human GW39 colon cancer tumours.[67] The highest dose, 10 mCi of ^{64}Cu–ATSM, increased survival to 135 d in 50% of animals bearing 7-day-old tumours, 6-fold longer than control animals' survival (20 d), with only transient leucopenia and thrombocytopenia but no overt toxicity. When a therapeutic level of ^{64}Cu–ATSM was combined with 2-deoxyglucose (2-DG), a glucose analog that selectively accumulates in cancer cells and interferes with energy metabolism resulting in cancer cell death, tumour growth in mice bearing EMT6 tumours was inhibited ~60% compared to untreated mice.[70]

Myocardial ischemia

Studies conducted using the Langendorff isolated perfused rat heart model, in which oxygen concentration can be controlled, showed that specific retention of Cu–ATSM is due to oxygen depletion.[37] Cu–ATSM was shown to have rapid washout from normally perfused isolated rat hearts whereas in ischemic hearts there was 3.5-fold retention of tracer in the ischemic tissue compared to healthy myocardium within 15 min of tracer administration. When compared to the distribution of a flow tracer 1-^{11}C-acetate, in the lower regions of flow (ischemia) ^{64}Cu–ATSM showed higher accumulation when compared to normal regions (Fig. 6).[71] In 2002, canine models of cardiac syndromes were used to further explore Cu–ATSM as a tracer for myocardial ischemia.[72] The first model resolved the effect of flow on washout and retention of the tracer and confirmed that Cu–ATSM was an effective tracer in the detection of global hypoxia. A second protocol demonstrated the usefulness of Cu–ATSM-PET for acute ischemic syndromes such as myocardial infarction when flow is limited. The data further demonstrated that there was no retention of Cu–ATSM in necrotic tissue, which has direct clinical implications if considering reperfusion therapies. The final protocol, where coronary artery stenosis was induced by a Teflon stent in the LAD coronary artery demonstrated the hypoxia imaging characteristics of Cu–ATSM when ischemia is induced without severe flow limitation.[72]

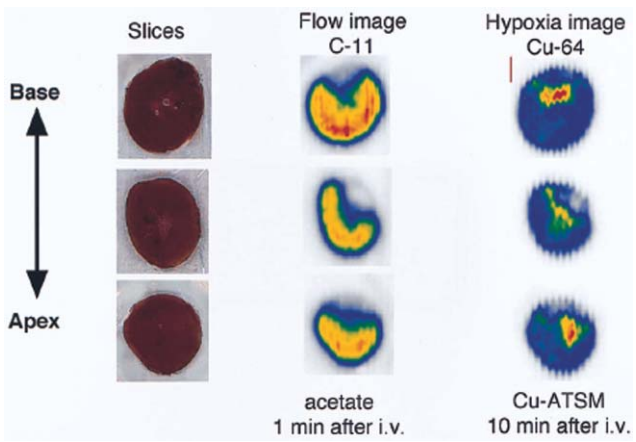

Fig. 6 *Ex vivo* imaging of a left anterior descending (LAD) coronary artery occluded rat heart model. The heart slices shown on the far left are digitized photographic images of the heart slices. In the middle is shown the distribution of 1-^{11}C-acetate. On the right is the distribution of ^{64}Cu–ATSM. Reprinted from *Nucl. Med. Biol.*, **26**, Fujibayashi *et al.*, Comparative imaging studies of ^{64}Cu-ATSM a hypoxia imaging agent and 1–^{11}C-acetate in an acute myocardial infarction model: Ex vivo imaging in rats, 117–121. Copyright (1999), with permission from Elsevier Inc.

New directions

As stated, the delineation of hypoxia in tissue has direct implications for the treatment of disease states such as cancer, stroke, and myocardial infarction. The definition of hypoxia depends on the disease examined, and the response to hypoxia differs at the systemic, local, and cellular levels. Although radiobiological hypoxia is typically defined at an oxygen concentration below <2.5 mmHg, cardiovascular or neurological tissue can be irreversibly damaged by reperfusion shock at oxygen concentration 10 to 100 times higher than that. As a consequence, there is a need to develop agents that can detect and treat hypoxia in different tissue types. To this end McQuade *et al.*, studied bis(selenosemicarbazone) complexes as hypoxia agents.[73] This study confirmed that subtle modification of bis(thiosemicarbazone) complexes and derivatives could alter the level of hypoxia at which preferential uptake is "switched on", but in general it showed that these selenium compounds added no benefit compared to the existing sulfur analogs and they do not appear to have been pursued further.

There have been a number of reports in the literature that thiosemicarbazone complexes could be used as a functional backbone for further derivatization as bifunctional chelators.[74–76] Recently, Cowley *et al.*, produced two new bifunctional chelators that are derivatives of the $ATSMH_2$ proligand, one with two phenyl carboxylate substituents on the exocyclic nitrogens and one with a single phenyl carboxylate.[77] The new proligands were tethered to the N-Boc-protected amino acids lysine and ornithine using solution and solid phase methods. The new amino acid conjugates formed copper complexes and were characterized by mass spectrometry and electronic spectroscopy. The second bifunctional chelator was conjugated to the tumour-targeting peptide octreotide to create a new $ATSMH_2$–octreotide conjugate. It remains to be seen if these new systems have the potential to be used as new targeted copper radiopharmaceuticals for imaging and therapy.

Limitations

^{18}F-FMISO, which contains a nitroimidazole moiety, is limited by slow kinetics and poor hypoxia to background ratios. The validity of Cu–ATSM as a hypoxia imaging agent has been demonstrated *in vitro*, *in vivo*, and in humans, but there is concern in regard to its ability to delineate hypoxia in all tumours, particularly prostate.[41,43] Some groups have reported data in prostate tumour lines that did not support the use of Cu–ATSM, at times finding a negative correlation of uptake to oxygen levels. Physiological changes caused by hypoxia could affect the cellular redox balance regardless of oxygen concentration. For example, as a defense mechanism in prostate cancer cells, the fatty acid synthesis (FAS) pathway harnesses its oxidizing power for improving the redox balance despite conditions of extreme hypoxia.[78] FAS is a multi-functional enzymatic protein involved in many stages of fatty acid biosynthesis including the conversion of malonyl-coA and acetate into palmitate. Although it is minimally expressed endogenously, FAS has been found to be over-expressed in prostate carcinomas as well as other cancers and increased levels have been shown to be indicative of aggressive and late-stage prostatic adenocarcinomas.[79] In a recent study, application of an inhibitor of FAS allowed the cells to overcome the ability of FAS to offset the redox balance of a hypoxic cell therefore increasing uptake of Cu–ATSM.[80] Inhibition of FAS with C75 resulted in a significant increase in ^{64}Cu–ATSM uptake into prostate tumour cells *in vitro* under anoxic conditions.

Conclusions

Cu–ATSM, labeled with a positron emitting isotope of copper (^{60}Cu, ^{61}Cu, ^{62}Cu or ^{64}Cu), has been shown to be selective for hypoxic cancers and ischemic myocardial tissue. Mechanistic studies examining the hypoxia-selectivity of Cu–ATSM have presented a number of mechanisms that explain the activity of this agent. More importantly, these studies clearly show that this agent can be finely tuned, by simple replacement of alkyl groups, to alter the biological properties of the agent. Clinical studies with this agent have shown non-invasive imaging data that is predictive of a cancer patients' response to conventional therapy after a simple and fast imaging session. Clearly, this agent has huge potential in individualized treatment planning for a cancer patient. Although Cu–ATSM is not perfect and may not be applicable for all cancer types, most notably prostate cancers, it stills holds exceptional potential as a hypoxic-PET agent and could make a significant impact in the fight against cancer.

Acknowledgements

The development of copper PET radiopharmaceuticals has been studied for decades in the United States, Europe and Japan. A large number of scientists from multiple disciplines and support staff have all been involved in the design and application of copper radiopharmaceuticals for the imaging of cancer and other diseases. We wish to acknowledge all of the dedicated people involved in the development of copper radiopharmaceuticals, which has now reached the point where agents have been translated to the clinic and are taking their place in the toolbox of molecular imaging. The development of ^{64}Cu–ATSM at Washington University School of Medicine was financially supported by the United States Department of Energy and the translation to the clinic was supported by the NCI/DCIDE program at the United States National Institutes of Health. Dr Vāvere's NIH/NRSA postdoctoral fellowship is supported by the National Institutes of Health (F32 CA110422–03). Dr Lewis' laboratory is supported by grants from the United States Department of Defense (PC040435) and the National Institutes of Health.

References

1 J. M. Brown, *Cancer Res.*, 1999, **59**, 5863–5870.
2 T. G. Graeber, C. Osmanian, T. Jacks, D. E. Housman, C. J. Koch, S. W. Lowe and A. J. Giaccia, *Nature*, 1996, **379**, 88–91.
3 M. Höckel, K. Schlenger, B. Aral, M. Mitze, U. Schäffer and P. Vaupel, *Cancer Res.*, 1996, **56**, 4509–4515.
4 D. Shweiki, A. Itin, D. Soffer and E. Keshet, *Nature*, 1992, **359**, 843–845.
5 J. L. Tatum, G. J. Kelloff, R. J. Gillies, J. M. Arbeit, J. M. Brown, K. S. C. Chao, J. D. Chapman, W. C. Eckelman, A. W. Fyles, A. J. Giaccia, R. P. Hill, C. J. Koch, M. C. Krishna, K. A. Krohn, J. S. Lewis, R. P. Mason, G. Melillo, A. R. Padhani, G. Powis, J. G. Rajendran, R. Reba, S. P. Robinson, G. L. Semenza, H. M. Swartz, P. Vaupel, D. Yang, B. Croft, J. Hoffman, G. Liu, H. Stone and D. Sullivan, *Int. J. Radiat. Biol.*, 2006, **82**, 699–757.
6 A. Fyles, M. Milosevic, D. Hedley, M. Pintille, W. Levein, L. Manchul and R. P. Hill, *J. Clin. Oncol.*, 2002, **20**, 620–687.

7 D. J. Terris, *Laryngoscope*, 2000, **110**, 697–707.
8 P. Vaupel, S. Briest and M. Höckel, *Semin. Oncol.*, 2001, **28**, 29–35.
9 J. R. Ballinger, *Semin. Nucl. Med.*, 2001, **31**, 321–329.
10 J. S. Lewis and M. J. Welch, *Q. J. Nucl. Med.*, 2001, **45**, 183–188.
11 A. R. Padhani, *Cancer Imaging*, 2005, **5**, 128–130.
12 A. R. Padhani, K. A. Krohn, J. S. Lewis and M. Alber, *Eur. Radiol.*, 2007, **17**, 861–872.
13 J. G. Rajendran and K. A. Krohn, *Radiol. Clin. N. Am.*, 2005, **43**, 169–187.
14 I. Serganova, J. L. Humm, C. C. Ling and R. Blasberg, *Clin. Cancer Res.*, 2006, **12**, 5260–5264.
15 J. S. Rasey, N. J. Nelson, L. K. Chin, M. L. Evans and Z. Grunbaum, *Radiat. Res.*, 1990, **122**, 301–308.
16 A. Nunn, K. Linder and H. W. Strauss, *Eur. J. Nucl. Med.*, 1995, **22**, 265–280.
17 J. G. Rajendran, D. C. Wilson, E. U. Conrad, L. M. Peterson, J. D. Bruckner, J. S. Rasey, L. K. Chin, P. D. Hofstrand, J. R. Grierson, J. F. Eary and K. A. Krohn, *Eur. J. Nucl. Med. Mol. Imaging*, 2003, **30**, 695–704.
18 J. G. Rajendran, D. A. Mankoff, F. O'Sullivan, L. M. Peterson, D. L. Schwartz, E. U. Conrad, A. M. Spence, M. Muzi, D. G. Farwell and K. A. Krohn, *Clin. Cancer Res.*, 2004, **10**, 2245–2252.
19 M. H. Cherk, S. S. Foo, A. M. Poon, S. R. Knight, C. Murone, A. T. Papenfuss, J. I. Sachinidis, T. H. Saunder, G. J. O'Keefe and A. M. Scott, *J. Nucl. Med.*, 2006, **47**, 1921–1926.
20 M. Piert, H.-J. Machulla, M. Picchio, G. Reischl, S. Ziegler, R. Kumar, H.-J. Wester, R. Beck, A. J. B. McEwan, L. I. Wiebe and M. Schwaiger, *J. Nucl. Med.*, 2005, **46**, 106–113.
21 P. J. Blower, J. S. Lewis and J. Zweit, *Nucl. Med. Biol.*, 1996, **23**, 957–980.
22 P. McQuade, D. J. Rowland, J. S. Lewis and M. J. Welch, *Curr. Med. Chem.*, 2005, **12**, 807–818.
23 *Handbook of Radiopharmaceuticals*, ed. M. J. Welch and C. S. Redvanly, John Wiley & Sons Ltd, Chichester, UK, 2003.
24 D. W. McCarthy, L. A. Bass, P. D. Cutler, R. E. Shefer, R. E. Klinkowstein, P. Herrero, J. S. Lewis, C. S. Cutler, C. J. Anderson and M. J. Welch, *Nucl. Med. Biol.*, 1999, **26**, 351–358.
25 D. W. McCarthy, R. E. Shefer, R. E. Klinkowstein, L. A. Bass, W. H. Margeneau, C. S. Cutler, C. J. Anderson and M. J. Welch, *Nucl. Med. Biol.*, 1997, **24**, 35–43.
26 T. Fukumara, K. Okada, H. Suzuki, R. Nakao, K. Mukai, F. Szelecsényi, Z. Kovacs and K. Suzuki, *Nucl. Med. Biol.*, 2006, **33**, 821–827.
27 N. G. Haynes, J. L. Lacy, N. Nayak, C. S. Martin, D. Dai, C. J. Mathias and M. A. Green, *J. Nucl. Med.*, 2000, **41**, 309–314.
28 X. Hou, U. Jacobsen and J. C. Jorgensen, *Appl. Radiat. Isot.*, 2002, **57**, 773–777.
29 L. P. Szajek, W. Meyer, P. Plascjak and W. C. Eckelman, *Radiochim. Acta*, 2005, **93**, 239–244.
30 F. Szelecsényi, G. Blessing and S. M. Qaim, *Appl. Radiat. Isot.*, 1993, **44**, 575–580.
31 S. K. Zeisler, R. A. Pavan, J. Orzechowski, R. Langlois, S. Rodrigue and J. E. van Lier, *J. Radioanal. Nucl. Chem.*, 2003, **257**, 175–177.
32 D. H. Petering, *Bioinorg. Chem.*, 1972, **1**, 255–271.
33 H. G. Petering, H. H. Buskirk and G. E. Underwood, *Cancer Res.*, 1964, **24**, 367–372.
34 M. A. Green, C. J. Mathias, M. J. Welch, A. H. McGuire, D. Perry, F. Fernandez-Rubio, J. S. Perlmutter, M. E. Raichle and S. R. Bergmann, *J. Nucl. Med.*, 1990, **31**, 1989–1996.
35 H. Taniuchi, Y. Fujibayashi, Y. Yonekura, J. Konishi and A. Yokoyama, *J. Nucl. Med.*, 1997, **38**, 1130–1134.
36 H. Young, P. Carnochan, J. Zweit, J. Babich, S. Cherry and R. Ott, *J. Nucl. Med.*, 1994, **21**, 336–341.
37 Y. Fujibayashi, H. Taniuchi, Y. Yonekura, H. Ohtani, J. Konishi and A. Yokoyama, *J. Nucl. Med.*, 1997, **38**, 1155–1160.
38 J. L. D. Dearling, J. S. Lewis, G. E. D. Mullen, M. T. Rae, J. Zweit and P. J. Blower, *Eur. J. Nucl. Med.*, 1998, **25**, 788–792.
39 J. L. J. Dearling, J. S. Lewis, G. E. D. Mullen, M. J. Welch and P. J. Blower, *JBIC, J. Biol. Inorg. Chem.*, 2002, **7**, 249–259.
40 J. S. Lewis, D. W. McCarthy, T. J. McCarthy, Y. Fujibayashi and M. J. Welch, *J. Nucl. Med.*, 1999, **40**, 177–183.
41 P. Burgman, J. A. O'Donoghue, J. S. Lewis, M. J. Welch, J. L. Humm and C. C. Ling, *Nucl. Med. Biol.*, 2005, **32**, 623–630.
42 J. S. Lewis, T. L. Sharp, R. Laforest, Y. Fujibayashi and M. J. Welch, *J. Nucl. Med.*, 2001, **42**, 655–661.
43 J. A. O'Donoghue, P. Zanzonico, A. Pugachev, B. Wen, P. Smith-Jones, S. Cai, E. Burnazi, R. D. Finn, P. Burgman, S. Ruan, J. S. Lewis, M. J. Welch, C. C. Ling and J. L. Humm, *Int. J. Radiat. Oncol., Biol., Phys.*, 2005, **61**, 1493–1502.
44 A. Obata, M. Yoshimoto, S. Kasamatsu, H. Naiki, S. Takamatsu, K. Kashikura, T. Furukawa, J. S. Lewis, M. J. Welch, H. Saji, Y. Yonekura and Y. Fujibayashi, *Nucl. Med. Biol.*, 2003, **30**, 529–534.
45 T. Tanaka, T. Furukawa, S. Fujieda, S. Kasamatsu, Y. Yonekura and Y. Fujibayashi, *Nucl. Med. Biol.*, 2006, **33**, 743–750.
46 H. Yuan, T. Schroeder, J. E. Bowsher, L. W. Hedlund, T. Wong and M. W. Dewhirst, *J. Nucl. Med.*, 2006, **47**, 989–998.
47 P. J. Blower, T. C. Castle, A. R. Cowley, J. R. Dilworth, P. S. Donnelly, E. Labisbal, F. E. Sowrey, S. J. Teat and M. J. Went, *Dalton Trans.*, 2003, 4416–4425.
48 P. J. Blower, J. R. Dilworth, R. I. Maurer, G. E. D. Mullen, C. A. Reynolds and Y. Zheng, *J. Inorg. Biochem.*, 2001, **85**, 15–22.
49 A. R. Cowley, J. R. Dilworth, P. S. Donnelly, E. Labisbal and A. Sousa, *J. Am. Chem. Soc.*, 2002, **124**, 5270–5271.
50 A. R. Cowley, J. R. Dilworth, P. S. Donnelly and J. M. White, *Inorg. Chem.*, 2006, **45**, 496–498.
51 J. L. J. Dearling, J. S. Lewis, M. J. Welch, D. W. McCarthy and P. J. Blower, *Chem. Commun.*, 1998, **22**, 2531–2533.
52 J. P. Holland, J. C. Green and J. R. Dilworth, *Dalton Trans.*, 2006, 783–794.
53 R. I. Maurer, P. J. Blower, J. R. Dilworth, C. A. Reynolds, Y. Zheng and G. E. D. Mullen, *J. Med. Chem.*, 2002, **45**, 1420–1431.
54 A. Obata, E. Yoshimi, A. Waki, J. S. Lewis, N. Oyama, M. J. Welch, H. Saji, Y. Yonekura and Y. Fujibayashi, *Ann. Nucl. Med.*, 2001, **15**, 499–504.
55 I. D. Baerga, R. P. Maickel and M. A. Green, *Int. J. Radiat. Appl. Instrum., Part B*, 1992, **19**, 697–701.
56 Y. Fujibayashi, K. Wada, H. Taniuchi, Y. Yonekura, J. Konishi and A. Yokoyama, *Biol. Pharm. Bull.*, 1993, **16**, 146–149.
57 T. C. Castle, R. I. Maurer, F. E. Sowrey, M. J. Went, C. A. Reynolds, E. J. L. McInnes and P. J. Blower, *J. Am. Chem. Soc.*, 2003, **125**, 10040–10049.
58 A. R. Cowley, J. Davis, J. R. Dilworth, P. S. Donnelly, R. Dobson, A. Nightingale, J. M. Peach, B. Shore, D. Kerr and L. Seymour, *Chem. Commun.*, 2005, **7**, 845–847.
59 N. Takahashi, Y. Fujibayashi, Y. Yonekura, M. J. Welch, A. Waki, T. Tsuchida, N. Sadato, K. Sugimoto and H. Itoh, *Ann. Nucl. Med.*, 2000, **14**, 323–328.
60 F. Dehdashti, P. W. Grigsby, M. A. Mintun, J. S. Lewis, B. A. Siegel and M. J. Welch, *Int. J. Radiat. Oncol., Biol., Phys.*, 2003, **55**, 1233–1238.
61 F. Dehdashti, M. A. Mintun, J. S. Lewis, J. Bradley, R. Govindan, R. Laforest, M. J. Welch and B. A. Siegel, *Eur. J. Nucl. Med. Mol. Imaging*, 2003, **30**, 844–850.
62 P. W. Grigsby, R. S. Malyapa, R. Higashikubo, J. K. Schwarz, M. J. Welch, P. C. Huettner and F. Dehdashti, *Mol. Imaging Biol.*, 2007, DOI: 10.1007/511307-007-0095-2.
63 C. Chao, W. R. Bosch, S. Mutic, J. S. Lewis, F. D. Dehdashti, M. A. Mintun, J. F. Demsey, C. A. Perez, J. A. Purdy and M. J. Welch, *Int. J. Radiat. Oncol., Biol., Phys.*, 2001, **49**, 1171–1182.
64 R. Laforest, F. Dehdashti, J. S. Lewis and S. W. Schwarz, *Eur. J. Nucl. Med. Mol. Imaging*, 2005, **32**, 764–770.
65 R. J. Myerson, A. K. Singh, H. M. Bigott, B. Cha, J. A. Engelbach, J. Kim, W. T. Lamoreaux, E. Moros, P. Novak, T. Sharp, W. Straube, M. J. Welch and M. Xu, *Int. J. Hyperthermia*, 2006, **22**, 93–115.
66 T. C. Rust and D. J. Kadrmas, *Phys. Med. Biol.*, 2006, **51**, 61–75.
67 J. S. Lewis, T. L. Buettner, J. M. Connett, Y. Fujibayashi and M. J. Welch, *Proc. Natl. Acad. Sci. USA*, 2001, **98**, 1206–1211.
68 A. Obata, S. Kasamatsu, J. S. Lewis, T. Furukawa, S. Takamatsu, J. Toyohara, T. Asai, M. J. Welch, S. G. Adams, H. Saji, Y. Yonekura and Y. Fujibayashi, *Nucl. Med. Biol.*, 2005, **32**, 21–28.
69 J. S. Lewis, J. M. Connett, J. R. Garbow, T. L. Buettner, Y. Fujibayashi, J. W. Fleshman and M. J. Welch, *Cancer Res.*, 2002, **62**, 445–449.
70 R. L. Aft, J. S. Lewis, F. Zhang, J. Kim and M. J. Welch, *Cancer Res.*, 2003, **63**, 5496–5504.
71 Y. Fujibayashi, C. S. Cutler, C. J. Anderson, D. W. McCarthy, L. A. Jones, T. Sharp, Y. Yonekura and M. J. Welch, *Nucl. Med. Biol.*, 1999, **26**, 117–121.
72 J. S. Lewis, P. Herrero, T. L. Sharp, J. A. Engelbach, Y. Fujibayashi, R. Laforest, A. Kovacs, R. J. Gropler and M. J. Welch, *J. Nucl. Med.*, 2002, **43**, 1557–1569.

73 P. McQuade, K. E. Martin, T. C. Castle, M. J. Went, P. J. Blower, M. J. Welch and J. S. Lewis, *Nucl. Med. Biol.*, 2005, **32**, 147–156.
74 C. J. Anderson, P. A. Rocque, C. J. Weinheimer and M. J. Welch, *Nucl. Med. Biol.*, 1993, **20**, 461–467.
75 Y. Fujibayashi, K. Matsumoto, Y. Arano, Y. Yonekura, J. Konishi and A. Yokoyama, *Chem. Pharm. Bull.*, 1990, **38**, 1946–1948.
76 D. W. McPherson, G. Umbricht and J. F. F. Knapp, *J. Labelled Compd. Radiopharm.*, 1990, **28**, 877.
77 A. R. Cowley, J. R. Dilworth, P. S. Donnelly, J. M. Heslop and S. J. Ratcliffe, *Dalton Trans.*, 2007, 209–217.
78 P. W. Hochachka, J. L. Rupert, L. Goldenberg, M. Gleave and P. Kozlowski, *Bioessays*, 2002, **24**, 749–757.
79 J. V. Swinnen, T. Roskams, S. Joniau, H. Van Poppel, R. Oyen, L. Baert, W. Heyns and G. Verhoeven, *Int. J. Cancer*, 2002, **98**, 19–22.
80 A. L. Vavere and J. S. Lewis, *J. Labelled Compd. Radiopharm.*, 2007, **50**, S437.

